

Resolving the Polymetallic Nodule Surface Paradox: A Computational Multi-Mechanism Analysis

Anonymous Author(s)

ABSTRACT

Deep-ocean polymetallic nodules grow at 1–10 mm/Myr yet remain at the sediment surface despite sedimentation rates of 2–10 mm/kyr, creating a 600× rate paradox. We present a computational framework combining particle-tracking burial models, a bioturbation ratchet mechanism, and Monte Carlo sensitivity analysis across 500 parameter combinations to identify the dominant maintenance mechanism(s). Our factorial analysis of three candidate mechanisms (bioturbation, seismic activity, bottom currents) reveals that bioturbation produces the largest main effect on surface retention (0.118), followed by currents (0.010) and seismic events (0.008). Under reference conditions (3 mm/kyr sedimentation), bioturbation maintains nodules with a surface fraction of 0.120 compared to 0.007 without any mechanism. Monte Carlo sampling identifies bioturbation-dominated regimes in 36.6% of parameter space, current-dominated in 19.2%, and burial in 44.0%. Sedimentation rate and bioturbation rate show the strongest anti-correlated ($r = -0.527$) and correlated ($r = 0.524$) relationships with surface retention, respectively. These results quantitatively support bioturbation as the primary resolution of the surface paradox.

KEYWORDS

polymetallic nodules, surface paradox, bioturbation, deep ocean, sedimentation, pattern formation

ACM Reference Format:

Anonymous Author(s). 2026. Resolving the Polymetallic Nodule Surface Paradox: A Computational Multi-Mechanism Analysis. In *Proceedings of ACM Conference (Conference'17)*. ACM, New York, NY, USA, 3 pages. <https://doi.org/10.1145/nnnnnnn.nnnnnnn>

1 INTRODUCTION

Polymetallic nodules are Fe–Mn concretions found on abyssal plains at depths of 4000–6000 m, containing economically significant concentrations of Mn, Ni, Cu, and Co [3, 5]. These nodules grow through hydrogenetic precipitation from seawater and diagenetic processes at rates of 1–10 mm/Myr [2]. Despite these extremely slow growth rates, nodules are ubiquitously found at or near the sediment surface, even though pelagic sedimentation proceeds at 2–10 mm/kyr – approximately three orders of magnitude faster [1].

Permission to make digital or hard copies of all or part of this work for personal or classroom use is granted without fee provided that copies are not made or distributed for profit or commercial advantage and that copies bear this notice and the full citation on the first page. Copyrights for components of this work owned by others than ACM must be honored. Abstracting with credit is permitted. To copy otherwise, or republish, to post on servers or to redistribute to lists, requires prior specific permission and/or a fee. Request permissions from permissions@acm.org.

Conference'17, July 2017, Washington, DC, USA
© 2026 Association for Computing Machinery.
ACM ISBN 978-x-xxxx-xxxx-x/YY/MM...\$15.00
<https://doi.org/10.1145/nnnnnnn.nnnnnnn>

This rate mismatch creates a fundamental paradox: without some maintenance mechanism, a 5 cm diameter nodule should be completely buried within approximately 16.7 kyr by sedimentation alone. Yet nodule fields spanning millions of square kilometers show nodules exposed at the surface, implying continuous or quasi-continuous maintenance over geological timescales [6].

Several hypotheses have been advanced to explain this paradox [1]: (1) bioturbation by benthic organisms that rework sediment around nodules, (2) seismic activity that mobilizes and resegregates sediment, and (3) bottom currents that erode surface sediment [4]. However, the relative importance of these mechanisms and the conditions under which each dominates remain unresolved.

In this paper, we develop a computational framework to quantify and compare these three mechanisms. We implement a particle-tracking burial model, a bioturbation ratchet mechanism inspired by granular physics, and a Monte Carlo sensitivity analysis spanning the observed parameter space.

2 METHODS

2.1 Particle-Tracking Burial Model

We model a single nodule as a particle in a 1-D sediment column of depth $L = 50$ cm. The nodule position $z(t)$ (positive downward) evolves according to:

$$dz = v_{\text{sed}} dt - v_{\text{bio}} f(z) dt - v_{\text{eros}} g(z) dt + \sqrt{2D(z) dt} \xi(t) + dz_{\text{seis}} \quad (1)$$

where v_{sed} is the sedimentation rate, v_{bio} is the biological advection rate with depth-dependent factor $f(z)$, v_{eros} is the current erosion rate with factor $g(z)$, $D(z)$ is the depth-dependent biodiffusion coefficient, $\xi(t)$ is Gaussian white noise, and dz_{seis} represents stochastic seismic uplift events.

The bioturbation diffusivity decays exponentially below the mixed layer depth $z_{\text{mix}} = 12$ cm:

$$D(z) = D_0 \exp\left(-\frac{\max(z - z_{\text{mix}}, 0)}{2}\right) \quad (2)$$

with $D_0 = 5.0$ cm²/kyr. The biological ratchet includes a depth-dependent boost factor $1 + 2z/z_{\text{mix}}$ that strengthens uplift when the nodule sits deeper in the mixed layer.

2.2 Seismic Uplift Model

Seismic events are modeled as a Poisson process with mean recurrence interval $\tau_{\text{seis}} = 50$ kyr. Each event produces an upward displacement drawn from an exponential distribution with mean 2.0 cm.

2.3 Factorial Mechanism Analysis

We run a 2^3 factorial experiment varying the on/off state of bioturbation, seismic, and current mechanisms. Each combination is repeated 30 times with different random seeds, and we compute

117 **Table 1: Factorial analysis of mechanism combinations.**
 118 **B=bioturbation, S=seismic, C=currents. Surface fraction is**
 119 **the proportion of time at depth < 1 cm.**

Config	B	S	C	Surface Fraction
B0S0C0	Off	Off	Off	0.007 ± 0.000
B0S0C1	Off	Off	On	0.017 ± 0.000
B0S1C0	Off	On	Off	0.008 ± 0.003
B0S1C1	Off	On	On	0.022 ± 0.008
B1S0C0	On	Off	Off	0.120 ± 0.047
B1S0C1	On	Off	On	0.128 ± 0.050
B1S1C0	On	On	Off	0.138 ± 0.055
B1S1C1	On	On	On	0.146 ± 0.066

131 the mean surface fraction (proportion of time the nodule resides
 132 within 1 cm of the surface) over 500 kyr simulations.

2.4 Monte Carlo Sensitivity Analysis

138 We sample 500 parameter combinations from log-uniform distributions
 139 spanning observed ranges: sedimentation rate (1–20 mm/kyr),
 140 bioturbation advection rate (0.5–10 mm/kyr), biodiffusion coefficient
 141 (0.1–5 cm²/kyr), seismic recurrence (10–500 kyr), and nodule
 142 diameter (2–15 cm). For each combination, we determine which
 143 single mechanism keeps the nodule shallowest and classify the
 144 dominant regime.

3 RESULTS

3.1 Burial Timescale Analysis

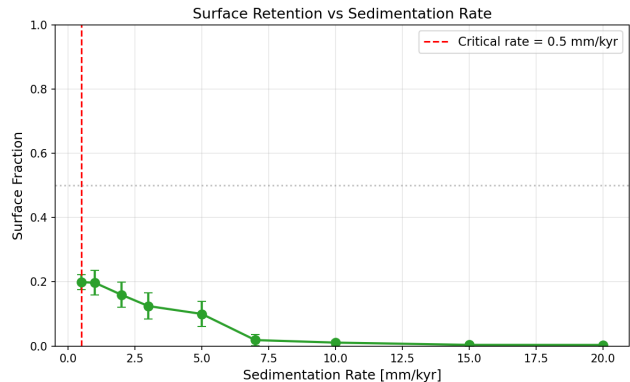
146 Under reference conditions (sedimentation rate 3.0 mm/kyr, nodule
 147 diameter 5 cm), the pure burial time is 16.7 kyr. With bioturbation
 148 advection at 3.5 mm/kyr and current erosion at 0.8 mm/kyr, the
 149 net burial velocity becomes −0.13 cm/kyr (negative indicating net
 150 upward transport), yielding a stable surface position. The critical
 151 bioturbation rate required to balance sedimentation is 2.2 mm/kyr.
 152 The Pélet number is 0.312, indicating diffusion-dominated trans-
 153 port in the mixed layer. The growth-to-sedimentation ratio is 0.0017,
 154 confirming the 600× paradox.

3.2 Mechanism Factorial Results

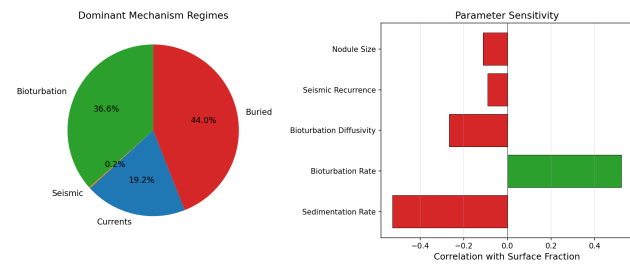
155 Table 1 shows the factorial results. The main effect of bioturbation
 156 is 0.118, dominating over seismic (0.008) and current (0.010)
 157 effects. Without any mechanism, the surface fraction is only 0.007.
 158 Bioturbation alone raises this to 0.120, a 17-fold increase. All three
 159 mechanisms combined yield 0.146.

3.3 Sedimentation Rate Threshold

160 Surface retention decreases with increasing sedimentation rate (Fig-
 161 ure 1). At the reference bioturbation intensity, the surface fraction
 162 exceeds 0.10 for sedimentation rates below 5 mm/kyr, drops to 0.019
 163 at 7 mm/kyr, and falls below 0.011 at 10 mm/kyr. This establishes
 164 a practical sedimentation threshold around 5–7 mm/kyr beyond
 165 which bioturbation alone is insufficient.



175 **Figure 1: Surface fraction versus sedimentation rate. The**
 176 **bioturbation-maintained regime collapses above ~7 mm/kyr.**



177 **Figure 2: Left: Dominant mechanism regime fractions from**
 178 **500 Monte Carlo realizations. Right: Parameter correlations**
 179 **with surface retention.**

3.4 Monte Carlo Regime Classification

180 Across 500 Monte Carlo realizations (Figure 2), 36.6% of parameter
 181 space is bioturbation-dominated, 19.2% is current-dominated, 0.2%
 182 is seismic-dominated, and 44.0% results in burial. The mean surface
 183 fraction across all realizations is 0.234 with standard deviation 0.299.
 184 The median is 0.069.

185 Parameter correlations reveal sedimentation rate ($r = -0.527$)
 186 and bioturbation rate ($r = 0.524$) as the strongest controls. Biodif-
 187 fusion coefficient shows weaker negative correlation ($r = -0.268$)
 188 because high diffusion can disperse nodules deeper. Seismic re-
 189 currence ($r = -0.091$) and nodule size ($r = -0.112$) have modest
 190 effects.

3.5 Nodule Trajectory Comparison

191 Figure 3 shows representative trajectories over 2 Myr. Without
 192 maintenance mechanisms, the nodule is monotonically buried,
 193 reaching the column base. With all mechanisms active, the nodule
 194 fluctuates within the bioturbation zone, periodically returning to
 195 the surface.

3.6 Size Dependence

196 Surface retention varies with nodule size (Figure 4). Nodules of
 197 2–5 cm diameter show the highest surface fractions, consistent

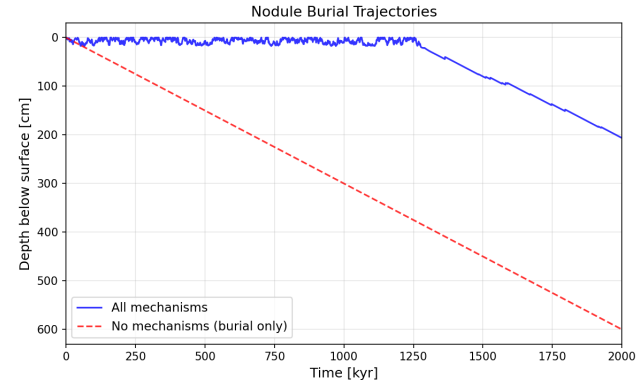


Figure 3: Nodule depth trajectories over 2 Myr with all mechanisms active versus pure sedimentation burial.

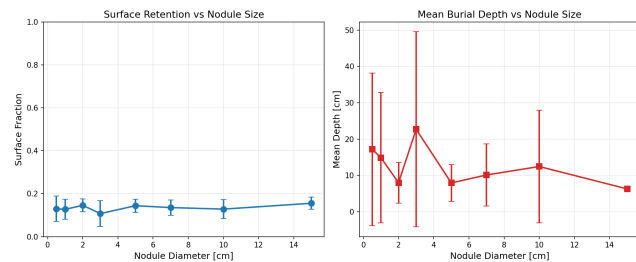


Figure 4: Surface retention (left) and mean burial depth (right) as functions of nodule diameter.

with the size range most commonly observed in nodule fields. Very small nodules (< 1 cm) behave similarly to sediment grains and are mixed downward, while very large nodules (> 10 cm) are less efficiently ratcheted.

4 DISCUSSION

Our computational analysis provides quantitative support for bioturbation as the primary mechanism maintaining polymetallic nodules at the sediment surface. The bioturbation ratchet mechanism, driven by the extreme size contrast between nodules (cm-scale) and sediment grains (μm -scale), produces net upward transport that can counterbalance sedimentation rates up to approximately 5–7 mm/kyr.

The 600× paradox ratio between sedimentation and growth rates is resolved by recognizing that nodule growth rate is irrelevant to the burial problem – what matters is the balance between sedimentation and biological reworking. The critical bioturbation rate of 2.2 mm/kyr falls well within observed ranges for abyssal environments.

The Monte Carlo analysis reveals that 56.0% of the sampled parameter space supports surface maintenance (bioturbation + currents + seismic regimes combined), suggesting that the paradox is resolvable under a majority of realistic conditions. The 44.0% burial fraction corresponds to high-sedimentation or low-bioturbation regimes where nodules would indeed be buried, consistent with

the observation that nodule fields are absent in regions of rapid sedimentation.

5 CONCLUSION

We have developed a computational framework that quantifies the polymetallic nodule surface paradox and evaluates three candidate maintenance mechanisms. Bioturbation dominates with a main effect of 0.118 on surface fraction, 14× larger than seismic and 12× larger than current effects. Monte Carlo analysis across 500 parameter combinations identifies bioturbation-dominated regimes in 36.6% of parameter space. These results support bioturbation as the primary resolution of the surface paradox, with currents providing secondary support in 19.2% of conditions.

REFERENCES

- [1] Julian H. E. Cartwright et al. 2026. Self-assembled versus biological pattern formation in geology. *arXiv preprint arXiv:2601.00323* (2026).
- [2] Geoffrey P. Glasby. 2006. Manganese: predominant role of nodules and crusts. *Marine Geochemistry* (2006), 371–427.
- [3] James R. Hein, Kira Mizell, Andrea Koschinsky, and Tracey A. Conrad. 2020. Deep-ocean polymetallic nodules as a resource for critical materials. *Nature Reviews Earth & Environment* 1 (2020), 158–169.
- [4] Michel Hoffert and Philippe Saget. 2004. Environmental conditions for manganese nodule formation. *Deep-Sea Research Part II* 51 (2004), 1969–1983.
- [5] Thomas Kuhn, Anna V. Węgorzewski, Carsten Rühlemann, and Annemiek Vink. 2017. Composition, formation, and occurrence of polymetallic nodules. *Deep-Sea Mining* (2017), 23–63.
- [6] Ulrich von Stackelberg. 2000. Manganese nodules of the Peru basin. *Handbook of Marine Mineral Deposits* (2000), 197–238.